Int J Cardiovasc Imaging (2010) 26:843–850
DOI 10.1007/s10554-010-9631-2

ORIGINAL PAPER

Combined optical coherence tomography and intravascular ultrasound radio frequency data analysis for plaque characterization. Classification accuracy of human coronary plaques in vitro

T. P. M. Goderie · G. van Soest · H. M. Garcia-Garcia · N. Gonzalo · S. Koljenović · G. J. L. H. van Leenders · F. Mastik · E. Regar · J. W. Oosterhuis · P. W. Serruys · A. F. W. van der Steen

Received: 24 December 2009 / Accepted: 5 April 2010 / Published online: 16 April 2010

Abstract This study was performed to characterize coronary plaque types by optical coherence tomography (OCT) and intravascular ultrasound (IVUS) radiofrequency (RF) data analysis, and to investigate the possibility of error reduction by combining these techniques. Intracoronary imaging methods have greatly enhanced the diagnostic capabilities for the detection of high-risk atherosclerotic plaques. IVUS RF data analysis and OCT are two techniques focusing on plaque morphology and composition. Regions of interest were selected and imaged with OCT and IVUS in 50 sections, from 14 human coronary arteries, sectioned post-mortem from 14 hearts of patients dying of non-cardiovascular causes. Plaques were classified based on IVUS RF data analysis (VH-IVUS^{TM}), OCT and the combination of those. Histology was the benchmark. Imaging with both modalities and coregistered histology was successful in 36 sections. OCT correctly classified 24; VH-IVUS 25, and VH-IVUS/OCT combined, 27 out of 36 cross-sections. Systematic misclassifications in OCT were intimal thickening classified as fibroatheroma in 8 cross-sections. Misclassifications in VH-IVUS were mainly fibroatheroma as intimal thickening in 5 cross-sections. Typical image artifacts were found to affect the interpretation of OCT data, misclassifying intimal thickening as fibroatheroma or thin-cap fibroatheroma. Adding VH-IVUS to OCT reduced the error rate in this study.

Keywords Intravascular imaging · Atherosclerosis · Plaque · OCT · IVUS · Histology

T. P. M. Goderie · G. van Soest (✉) · H. M. Garcia-Garcia · N. Gonzalo · F. Mastik · E. Regar · P. W. Serruys · A. F. W. van der Steen
Thorax Center Biomedical Engineering, Erasmus MC Rotterdam, Ee23.02, PO Box 2040, 3000 CA Rotterdam, The Netherlands
e-mail: g.vansoest@erasmusmc.nl

S. Koljenović · G. J. L. H. van Leenders · J. W. Oosterhuis
Department of Pathology, Erasmus MC Rotterdam, Rotterdam, The Netherlands

A. F. W. van der Steen
Interuniversity Cardiology Institute of the Netherlands, Utrecht, The Netherlands

Introduction

Pathology studies have demonstrated that most of acute coronary syndromes originate from vulnerable plaques [1–5]. Such lesions have a mechanically weak cap, consisting of a thin fibrotic layer that is infiltrated by macrophages, overlying a lipid-rich necrotic core [1, 6, 7]. The current challenge is to specifically identify plaques that exhibit these characteristics in vivo [8]. Clinical diagnosis may benefit from complementary information gathered by different imaging modalities, as the sensitivities of the

technologies to specific aspects of the anatomy may differ and confounders are likely to be technology-specific [9–14].

Grayscale Intravascular Ultrasound (IVUS) has since long been a standard diagnostic tool in cath labs worldwide, and intravascular Optical Coherence Tomography (OCT) looks set to become one as well [12, 15–18]. IVUS radio frequency (RF) data analysis adds plaque composition information to the grayscale images, which may help to distinguish high-risk lipid-rich necrotic plaques from other types of plaques [19–21]. IVUS RF data aims to provide quantitative information on plaque composition classifying plaque as fibrotic, fibrofatty, necrotic core or dense calcium, based on spectral analysis of the RF signal [11]. Criteria have been formulated to detect thin-cap fibroatheroma (TCFA), but as a standalone technique it is not able to recognize this type of lesion because of its limited resolution (>250 μm) [14, 22–24].

Optical coherence tomography (OCT) generates real time tomographic images from backscattered infrared light with a high resolution (10–15 μm axial) [12, 25]. Its resolution allows direct imaging of a thin fibrous cap. Limitations are the small depth of penetration (approximately 1–1.5 mm) and the need to clear blood from the imaged artery [12]. This latter issue is relieved by the new high-speed intracoronary imaging systems requiring only a short flush for full imaging of a coronary artery [15].

The aim of this study was to compare the ability of OCT and VH-IVUS to classify plaque and to assess the performance of a combination of the two modalities to identify different plaque types, with an eye to future development of new devices. While a few in-vivo studies have been published [14, 26], in this work we present the first comparison between VH-IVUS and OCT, using histology as a benchmark.

Methods

Study population

Between June 2007 and January 2008, 14 coronary arteries have been collected from 14 human hearts acquired during autopsy (57% men, 12 left anterior descending arteries, 2 right coronary arteries, mean age 64) at the Department of Pathology of the Erasmus MC. All patients died of non-coronary causes. Permission to use autopsy material for scientific study was obtained from the relatives. This study was approved by the local institutional review board.

Tissue preparation and data acquisition

Atherosclerotic human coronary artery segments were excised from the heart and imaged within 36 h postmortem. During the excision all side branches were closed with sutures. The arteries were mounted between 2 sheaths in a water tank filled with physiological saline. A water column system, also containing physiological saline solution, was connected to the proximal sheath, to pressure-load the vessel. The vessels were pressurized to 100 mmHg to close up remaining leakages.

The vessels were imaged with OCT (M2-CV and ImageWire 2 catheters; Lightlab Imaging, Westford, MA) and IVUS (In-vision Gold; Eagle-Eye^{TM} 20 MHz catheters; Volcano, Rancho Cordova, CA). Regions of interest (ROIs) were selected based on the presence of plaque and plaque size by grayscale IVUS. ROIs were marked with a needle. After imaging the needle was replaced by a suture.

ROIs were first imaged with the IVUS-system, followed by OCT. The vessels were pressurized to 100 mmHg for imaging. For IVUS, the vessels were kept at room temperature 20 ± 2°C; OCT was performed at 37°C [27, 28].

After imaging, the artery sections were pressure fixed at 100 mmHg in formaldehyde for 24 h at room temperature, and subsequently stored in formaldehyde at 4°C for further processing. Vessels were partially decalcified for 24 h in formic acid [29]. After fixation and decalcification, sutures marking the imaged cross-sections were replaced by ink dots. The tissue was embedded in paraffin and sectioned at the ink markers for histological staining. Each imaged cross-section was stained with Hematoxylin-Eosin (H&E), Picrosirius red, Elastic van Gieson (EvG) and immunohistochemical stain CD68.

Data classification

Plaques were characterized in the images acquired with the two modalities, as well as in histology. As histological tissue slices are much thinner (5 μm) than the thickness sampled by OCT (25 μm) or IVUS (~200 μm) [30, 31] there is an unavoidable

sampling error. Imaged cross-sections that were obviously mismatched with histology, based on anatomical features (such as plaque shape, presence of small side branches) were removed from the data set before analysis.

OCT

Classification of OCT was based on characteristics as mentioned in Table 1 by two experienced OCT readers [12, 32–35]. Because of the limited depth of imaging and the limited penetration in OCT, tissue types could not be expressed as percentages of the intima like in VH-IVUS, but had to be based on qualitative assessment of the visible part of the OCT image. In cross-sections with no visible cap, defined by a transition of signal from homogeneous signal rich to otherwise, the cross-section was classified as intimal thickening. In presence of a cap the dominant tissue type behind the cap was used to assess lesion type.

VH-IVUS

In this article, we will refer to IVUS RF data analysis as VH-IVUS (Volcano, Rancho Cordova, CA, USA), since we used that technology specifically. VH-IVUS constructs tissue maps that classify plaque into four major components (fibrous—green, fibrofatty—light green, NC—red, and dense calcium—white) [36]. Data were acquired, and B-mode images were reconstructed from the RF data by customized software (pcVH 2.2, Volcano Corporation), which allows a semiautomatic detection of the lumen and the media-adventitia borders and provides the compositional parameters. VH cross-sections were quantitatively measured and were classified as one of the categories described in Table 1 by an experienced analyst that was blind for pathological and OCT findings [32, 33, 37].

Combined OCT and VH

After independent analysis of each technique, plaque type was evaluated in a side-by-side visual assessment of VH-IVUS and OCT cross-sections. The criteria in Table 1 were applied for both techniques. If the classifications diverged between VH-IVUS and OCT, signal rich regions in OCT overruled VH-IVUS tissue characterization. In signal poor regions in OCT, VH-IVUS overruled OCT. This choice was made because a loss of OCT signal can occur due to artifacts, whereas artifacts are unlikely to cause a gain in image intensity.

Histology

Histological cross-sections were characterized by two observers blinded for the VH-IVUS and OCT results. Characterization was done by making a map of all the cross-sections, with color coding for different types of tissue, separating fibrotic tissue, lipid pool, necrotic core and dense calcium. In case of disagreement between the two pathologists, pathologist 1 and pathologist 2 re-evaluated the slides and reached a consensus diagnosis. Classification of cross-sections was done based on the American Heart Association (AHA) classification of 1995 [32, 38], distinguishing four categories of advanced lesions: fibroatheroma (FA; type IV and Va), intimal thickening (IT; type Vb), fibrocalcific (FC; type Vc), and complicated lesions (type VI; comprising thrombus, rupture, and hemorrhage).

Table 1 Criteria for plaque characterization in VH and OCT

Lesion type	Brief description in VH [37]	Brief description in OCT [34, 35]
Intimal thickening	Plaque with <10% of NC and <10% of calcified tissue	Homogeneous signal-rich region
Fibroatheroma	Plaque with >10% of confluent NC	Heterogeneous signal poor regions poorly delineated
Fibrocalcific plaque	>10% of confluent DC with <10% of confluent NC	Homogeneous sharply delineated signal poor regions
Complicated lesion	–	Rupture: discontinuous cap over visible cavity
		Thrombus: irregular mass protruding into lumen

NC necrotic core, *DC* dense calcium. No criteria exist for complicated lesions seen with VH; of the complicated lesions defined in the AHA classification, rupture and thrombus (but not hemorrhage) are defined for OCT. Fibroatheromas often also contain calcifications; lesions that contained both significant necrotic core and calcification, were categorized as fibroatheroma

Results

OCT and VH-IVUS imaging, with positively matched histology, succeeded in 36 cross-sections in 9 of 14 vessels. In 5 vessels, imaging with either technique, or analysis of the acquired data, failed. Reasons for failure were inability to pass the IVUS catheter through the artery (VH-IVUS); catheter placement against the lumen wall, complicating border definition (VH-IVUS); and inability to image the full cross-section (OCT). A number of imaged cross-sections were removed from the data set because of anatomical mismatch (5 cases) or due to loss of the marker needle after imaging (1 case).

Table 2 lists the results of the comparison between histology and OCT; VH; and VH and OCT combined for the 36 cross-sections. OCT correctly identified the lesion in 24 cross-sections, VH-IVUS in 25, and OCT and VH-IVUS combined in 27. Figure 1 shows misclassifications separated per plaque type; only misclassifications occurring more than twice are included. Systematic misclassifications were mainly IT classified as FA (8 times) in OCT; FA as IT (5 times) in VH-IVUS; and FA as IT (4 times) in OCT and VH-IVUS combined.

Discussion

Results of this study

The results in Table 2 demonstrate that the classifications by both OCT and VH-IVUS agree with histology in most cases. Figure 2 illustrates a representative example, where both OCT and VH detect a fibroatheroma (with calcification), which is in accordance with the histological classification. We found that plaque classification by OCT and VH-IVUS combined was successful in more cross-sections than either technology alone, although the differences are small.

We encountered a high dropout rate of 28% (14 out of 50 lesions). Most of these were caused by problems during data acquisition, as presented in the Results section. About one third of the dropouts were removed from the data set because of a bad anatomical match between image data and histology, caused by the different slice thicknesses sampled by the imaging techniques and histology. This category of dropouts may be reduced by adopting a more elaborate histology slicing protocol, sampling 0.5–1 mm around every marked site [30].

Table 2 shows that the imaging modalities classify some lesions more reliably than others. Some features stand out in particular. We separate the discussion if these findings per technology.

Table 2 Classification and misclassification by OCT, VH-IVUS and OCT/VH-IVUS combined, compared to plaque type by histology, in 36 cross-sections

	OCT		VH		OCT/VH	
IT	19	9	24	4	25	3
	2	6	7	1	6	2
FiCa	1	0	0	1	0	1
	1	34	1	34	1	34
FA	4	2	1	5	2	4
	9	21	3	27	2	28
Compl.	0	1	0	1	0	1
	0	35	0	35	0	35

plaque type	technology	
	TP	FN
	FP	TN

Given are true and false positives and negatives as indicated in the matrix on the right. *IT* Intimal thickening, *FC* Fibrocalcific, *FA* Fibroatheroma, *Compl.* Complicated lesion

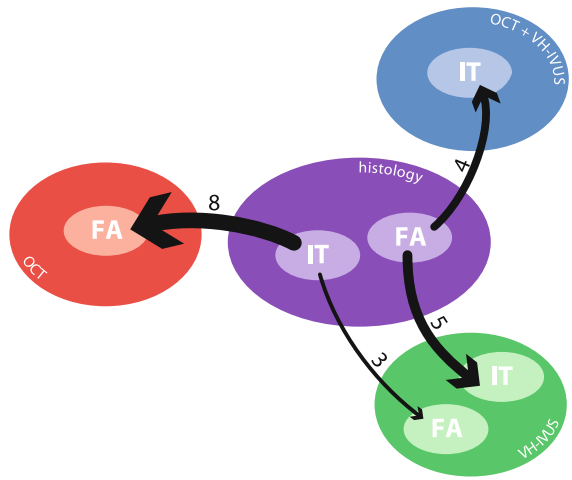

Fig. 1 Chart of misclassifications; the *arrows* indicate the misclassification of histology-characterized lesions by the respective imaging techniques. The thickness of the arrow represents the frequency in the data set, which is also indicated by the numbers on the arrows. For example: of the lesions that were identified as IT in histology, 8 were interpreted as FA in OCT. Only misclassifications occurring more than twice are included in the figure. *IT* intimal thickening, *FA* fibroatheroma

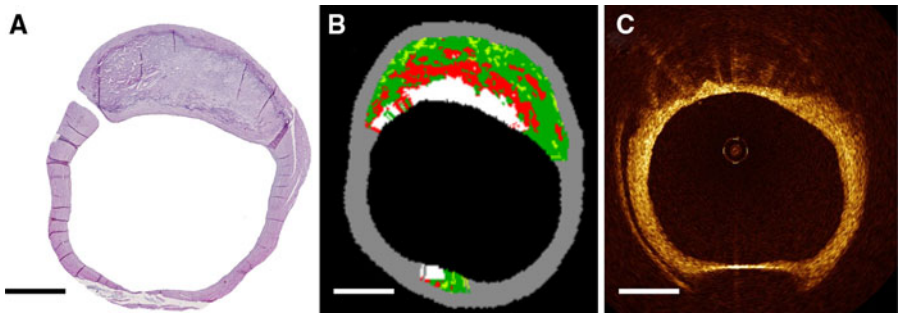

Fig. 2 **a** Histology of a calcified fibroatheroma. **b** Corresponding VH-IVUS classified as calcified fibroatheroma. **c** Corresponding OCT classified as calcified fibroatheroma. The needle used to mark the site can be seen in the bright feature at 6 o'clock in OCT, as well as in the appearance of dense calcium in that location in VH-IVUS

OCT

OCT characterized 24 out of 36 lesions correctly. A large fraction of misclassifications were false-positives for FA (9 out of 30 non-FA plaques). Figure 1 shows that 8 of these were IT in histology, which should appear homogeneously bright in OCT. Imaging artifacts can lead to signal loss and apparent heterogeneity in the image, leading to misclassification of a stable lesion as a potentially unstable one. We have not performed a systematic study of OCT artifacts, but found several examples in which shadowing by impurities in or on the catheter caused diffuse signal-poor sectors [39], as well as dark areas apparently associated with catheter position relative to the vessel wall.

Of the lesions classified as FAs by OCT, three were measured to have a thin fibrous cap (<65 μm). One of these apparent TCFAs was a complicated lesion with intraplaque hemorrhage, for which no OCT criterion exists. No actual TCFAs were found by histology.

VH-IVUS

VH-IVUS correctly classified 25 out of 36 lesions. All but one of the FA plaques were interpreted as IT, making up half of the misclassifications, and indicating a high false-negative rate for FA (1 out of 6 correctly classified). The reverse (IT interpreted as FA) was also observed three times. In VH-IVUS, classification is an automatic process, giving less inter-observer variability, but complicating the explanation of errors in VH-IVUS compared to histology.

VH tissue characterization depends strongly on correct drawing of lumen and adventitial borders. The lumen border was not always clear in our data because of proximity of the catheter to the vessel wall, while part of the adventitial border was sometimes obscured by dorsal shadowing of calcium. Identification of the lumen border is facilitated in vivo by tissue and pullback motion. In our study, cross-sections were imaged in vitro, creating a possible disadvantage for this technology.

OCT + VH combined

Combining the image data of both techniques yields the highest rate of successful classifications: 27 out of 36, although the difference with either technique alone is small. As with VH-IVUS alone, a high false-negative rate for FA is observed (2 out of 6 correctly classified). The systematic error in OCT classification (high false-positive rate for FA) has been reduced.

In 15 cases, classifications from both techniques diverged. Out of these, the combined classification followed VH in 13 cases (using the rule: in OCT-signal rich regions, OCT overruled VH-IVUS tissue characterization; in OCT-signal poor regions, VH-IVUS overruled OCT). This means that five correct OCT classifications were reversed by VH-IVUS: overall, VH added useful information to OCT, particularly in cases where OCT misclassified IT plaques as FA. Criteria for classifying VH-IVUS combined with OCT have not been independently validated and can likely be improved using larger datasets.

Comparison with literature

Manfrini et al. [38] were the first to apply the American Heart Association criteria to lesion classification with OCT. That study showed a sensitivity of 45% for FA, 68% for calcified lesions and 86% for fibrotic lesions. The limited size of our study did not permit reliable calculation of sensitivities and specificities, but a rough comparison can be made. Our results suggest a similar sensitivity for the detection of FA (4/6 correctly classified; 67%), and a lower one for fibrotic plaque, categorized in our study as intimal thickening (19/28 correctly classified; 68%).

Recent studies in OCT showed difficulties detecting TCFA in OCT and in characterizing plaques with OCT [14, 38]. Misclassifications were reported as a result of limited penetration depth, problems in distinguishing lipid pool from calcifications and vice versa, or heterogeneity of necrotic cores, consisting of necrotic debris and calcifications [12–14, 26, 38]. Heterogeneity inherently introduces a degree of arbitrariness in plaque classification. The accuracy of OCT plaque classification may be increased with the use of quantitative analysis techniques for tissue characterization [40, 41].

Diethrich et al. [37] report a sensitivity of 89% of VH-IVUS for detection of IT, which is in agreement with our results (24/28 correctly identified, 86%). We find fewer FAs (1/6 identified, 16%) than expected by Diethrich's study (54%). Our sample size is too small to draw definitive conclusions, however our results appear to be more in line with previous findings of Granada who reported lower sensitivities and specificities [42].

Our OCT data show a relatively high number of false-positives for FA: fibrous or fibrocalcific lesions were classified as FA in 9 cross-sections; three of these were measured to have a thin cap. A recent study describes the low incidence of histology-derived TCFA and FA (1.5% and 10.5% of advanced lesions, respectively) [43]. In the light of these data on natural incidence of FA and especially of TCFA, and our observed false-positive rate, the positive predictive value of OCT, an important parameter in rare incidence, could be small for these clinically significant plaque types. Since the group of non-TCFAs appears to be 98.5% in advanced lesions, the finding of a TCFA in OCT must be regarded with caution, and corroborated with other evidence if possible. An in-vivo study by Sawada et al. [14] combined VH-IVUS and OCT for detection of TCFA. Only lesions classified as TCFA both in OCT and in VH-IVUS were considered real TCFAs. This definition is indeed a sensible one, as the resolution of VH-IVUS is insufficient per se to identify thin caps, and OCT is seen to suffer from many false positives.

Limitations of this study

The conclusions to be drawn from this study have to remain tentative for three reasons. The first of those is the limited size of our data set. We have opted to discuss our results in a qualitative fashion, looking for repetitive features in the classification performance of the different techniques as illustrated in Fig. 1. As mentioned above, reliable calculation of sensitivity and specificity for the classification of plaque type is not warranted by our small set of samples.

A second observation is that our data set, containing predominantly fibrotic lesions, is more homogeneous than expected, based on the literature [33]. We speculate that our selection of patients dying from non-cardiac causes may have skewed the plaque type population in this study. This fact should be borne in mind when extrapolating our results to the patient characteristics typically found in a cardiology clinic. Clinical applicability of our results is inherently limited by the in vitro setting of our experiments: the absence of cardiac motion, blood and body temperature (in the case of VH-IVUS). Body temperature has a documented effect on the OCT signal [28], and was maintained during OCT acquisition.

A final consideration relates to the definition of classification criteria. The criteria for combined OCT + IVUS analysis, in case of disagreement between the two, are based on the physics of the imaging techniques, but have not been validated in an independent study. In addition, no classification criteria exist for complicated lesions in VH, and only for the AHA type VI subsets of thrombus and ruptured plaques in OCT. We found only one complicated plaque, containing hemorrhage, which could—by definition—not be identified. Had we found several complicated plaques, our results would have been noticeably biased.

Conclusion

In conclusion, we have compared plaque classification by OCT, VH-IVUS, and a combination of both. The combined data yielded more correct classifications than either technique alone, although differences were small. In vitro studies with larger sample sizes are needed to assess the added value of combining OCT and VH-IVUS. VH-IVUS showed a high-false-negative rate for fibroatheroma, while in the OCT data, we found a large number of false positives for this plaque type. Our findings merit a more thorough investigation of OCT artifacts, as we have seen them to significantly bias image interpretation.

References

1. Schaar JA, Muller JE, Falk E et al (2004) Terminology for high-risk and vulnerable coronary artery plaques. Report of a meeting on the vulnerable plaque, June 17 and 18, 2003, Santorini, Greece. Eur Heart J 25:1077–1082
2. Kolodgie FD, Virmani R, Burke AP et al (2004) Pathologic assessment of the vulnerable human coronary plaque. Heart 90:1385–1391
3. Granada JF, Kaluza GL, Raizner AE, Moreno PR (2004) Vulnerable plaque paradigm: prediction of future clinical events based on a morphological definition. Catheter Cardiovasc Interv 62:364–374
4. Muller JE, Abela GS, Nesto RW, Tofler GH (1994) Triggers, acute risk factors and vulnerable plaques: the lexicon of a new frontier. J Am Coll Cardiol 23:809–813
5. Davies MJ, Thomas AC (1985) Plaque fissuring—the cause of acute myocardial-infarction, sudden ischemic death, and crescendo angina. Br Heart J 53:363–373
6. Virmani R, Burke AP, Farb A, Kolodgie FD (2006) Pathology of the vulnerable plaque. J Am Coll Cardiol 47:C13–C18
7. Falk E, Shah PK, Fuster V (1995) Coronary plaque disruption. Circulation 92:657–671
8. Waxman S, Ishibashi F, Muller JE (2006) Detection and treatment of vulnerable plaques and vulnerable patients—novel approaches to prevention of coronary events. Circulation 114:2390–2411
9. Schaar JA, de Korte CL, Mastik F et al (2003) Characterizing vulnerable plaque features with intravascular elastography. Circulation 108:2636–2641
10. Baldewsing RA, Danilouchkine MG, Mastik F, Schaar JA, Serruys PW, van der Steen AFW (2008) An inverse method for imaging the local elasticity of atherosclerotic coronary plaques. IEEE Trans Inf Technol Biomed 12:277–289
11. Nair A, Kuban BD, Tuzcu EM, Schoenhagen P, Nissen SE, Vince DG (2002) Coronary plaque classification with intravascular ultrasound radiofrequency data analysis. Circulation 106:2200–2206
12. Jang IK, Bouma BE, Kang DH et al (2002) Visualization of coronary atherosclerotic plaques in patients using optical coherence tomography: comparison with intravascular ultrasound. J Am Coll Cardiol 39:604–609
13. Kawasaki M, Bouma BE, Bressner J et al (2006) Diagnostic accuracy of optical coherence tomography and integrated backscatter intravascular ultrasound images for tissue characterization of human coronary plaques. J Am Coll Cardiol 48:81–88
14. Sawada T, Shite J, Garcia-Garcia HM et al (2008) Feasibility of combined use of intravascular ultrasound radiofrequency data analysis and optical coherence tomography for detecting thin-cap fibroatheroma. Eur Heart J 29:1136–1146
15. Yun SH, Tearney GJ, Vakoc BJ et al (2006) Comprehensive volumetric optical microscopy in vivo. Nat Med 12:1429–1433
16. Nissen SE, Yock P (2001) Intravascular ultrasound: novel pathophysiological insights and current clinical applications. Circulation 103:604–616
17. Kubo T, Imanishi T, Takarada S et al (2007) Assessment of culprit lesion morphology in acute myocardial infarction—ability of optical coherence tomography compared with intravascular ultrasound and coronary angioscopy. J Am Coll Cardiol 50:933–939
18. Serruys PW, Garcia-Garcia HM, Regar E (2007) From postmortem characterization to the in vivo detection of thin-capped fibroatheromas: the missing link toward percutaneous treatment: what if diogenes would have found what he was looking for? J Am Coll Cardiol 50:950–952
19. Moore MP, Spencer T, Salter DM et al (1998) Characterisation of coronary atherosclerotic morphology by spectral analysis of radiofrequency signal: in vitro intravascular ultrasound study with histological and radiological validation. Heart 79:459–467
20. Komiyama N, Berry GJ, Kolz ML et al (2000) Tissue characterization of atherosclerotic plaques by intravascular ultrasound radiofrequency signal analysis: an in vitro study of human coronary arteries. Am Heart J 140:565–574
21. Murashige A, Hiro T, Fujii T et al (2005) Detection of lipid-laden atherosclerotic plaque by wavelet analysis of radiofrequency intravascular ultrasound signals: in vitro validation and preliminary in vivo application. J Am Coll Cardiol 45:1954–1960
22. Nair A, Calvetti D, Vince DG (2004) Regularized autoregressive analysis of intravascular ultrasound backscatter: improvement in spatial accuracy of tissue maps. IEEE Trans Ultrason Ferroelectr Freq Control 51:420–431
23. Rodriguez-Granillo GA, Garcia-Garcia HM, Mc Fadden EP et al (2005) In vivo intravascular ultrasound-derived thin-cap fibroatheroma detection using ultrasound radiofrequency data analysis. J Am Coll Cardiol 46:2038–2042
24. Garcia-Garcia HM, Goedhart D, Schuurbiers JCH et al (2006) Virtual histology and remodelling index allow in vivo identification of allegedly high-risk coronary plaques

in patients with acute coronary syndromes: a three vessel intravascular ultrasound radiofrequency data analysis. EuroIntervention 2:338–344
25. Huang D, Swanson EA, Lin CP et al (1991) Optical coherence tomography. Science 254:1178–1181
26. Gonzalo N, Serruys PW, Barlis P, Ligthart J, Garcia-Garcia HM, Regar E (2010) Multi-modality intra-coronary plaque characterization: a pilot study. Int J Cardiol 138:32–39
27. Schaar JA, de Korte CL, Mastik F, van der Steen AF (2002) Effect of temperature increase and freezing on intravascular elastography. Ultrasonics 40:879–881
28. van der Meer FJ, Faber DJ, Cilesiz I, van Gemert MJ, van Leeuwen TG (2006) Temperature-dependent optical properties of individual vascular wall components measured by optical coherence tomography. J Biomed Opt 11:041120
29. Friedrich GJ, Moes NY, Muhlberger VA et al (1994) Detection of intralesional calcium by intracoronary ultrasound depends on the histologic pattern. Am Heart J 128:435–441
30. Bruining N, Verheye S, Knaapen M et al (2007) Three-dimensional and quantitative analysis of atherosclerotic plaque composition by automated differential echogenicty. Catheter Cardiovasc Interv 70:968–978
31. Rieber J, Meissner O, Babaryka G et al (2006) Diagnostic accuracy of optical coherence tomography and intravascular ultrasound for the detection and characterization of atherosclerotic plaque composition in ex-vivo coronary specimens: a comparison with histology. Coron Artery Dis 17:425–430
32. Stary HC, Chandler AB, Dinsmore RE et al (1995) A definition of advanced types of atherosclerotic lesions and a histological classification of atherosclerosis. A report from the committee on vascular lesions of the council on arteriosclerosis, American heart association. Circulation 92:1355–1374
33. Virmani R, Kolodgie FD, Burke AP, Farb A, Schwartz SM (2000) Lessons from sudden coronary death—a comprehensive morphological classification scheme for atherosclerotic lesions. Arterioscler Thromb Vasc Biol 20: 1262–1275
34. Yabushita H, Bourna BE, Houser SL et al (2002) Characterization of human atherosclerosis by optical coherence tomography. Circulation 106:1640–1645
35. Tanaka A, Imanishi T, Kitabata H et al (2008) Morphology of exertion-triggered plaque rupture in patients with acute coronary syndrome: an optical coherence tomography study. Circulation 118:2368–2373
36. Nair A, Margolis MP, Kuban BD, Vince DG (2007) Automated coronary plaque characterization with intravascular ultrasound backscatter: ex vivo validation. EuroIntervention 3:113–120
37. Diethrich EB, Pauliina Margolis M, Reid DB et al (2007) Virtual histology intravascular ultrasound assessment of carotid artery disease: the carotid artery plaque virtual histology evaluation (CAPITAL) study. J Endovasc Ther 14:676–686
38. Manfrini O, Mont E, Leone O et al (2006) Sources of error and interpretation of plaque morphology by optical coherence tomography. Am J Cardiol 98:156–159
39. Bezerra HG, Costa MA, Guagliumi G et al (2009) Intracoronary optical coherence tomography: a comprehensive review: clinical and research applications. J Am Coll Cardiol Interv 2:1035–1046
40. van Soest G, Goderie TPM, Regar E et al (2010) Atherosclerotic tissue characterization in vivo by optical coherence tomography attenuation imaging. J Biomed Opt 15:011105
41. Xu C, Schmitt JM, Carlier SG, Virmani R (2008) Characterization of atherosclerosis plaques by measuring both backscattering and attenuation coefficients in optical coherence tomography. J Biomed Opt 13:034003
42. Granada JF, Wallace-Bradley D, Win HK et al (2007) In vivo plaque characterization using intravascular ultrasound-virtual histology in a porcine model of complex coronary lesions. Arterioscler Thromb Vasc Biol 27: 387–393
43. Cheruvu PK, Finn AV, Gardner C et al (2007) Frequency and distribution of thin-cap fibroatheroma and ruptured plaques in human coronary arteries: a pathologic study. J Am Coll Cardiol 50:940–949